

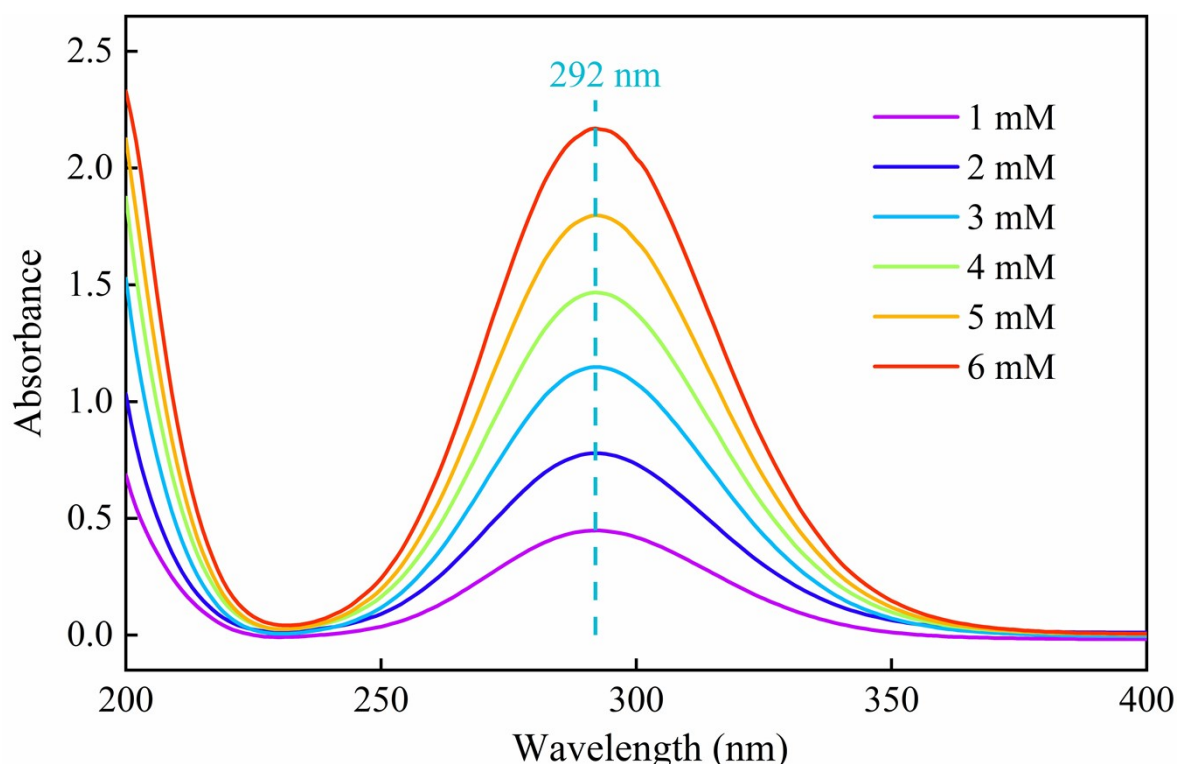
Supporting Information

Acidic chloride electrolyte mediates the high conversion ratio of CO₂-to-C₂H₄ and direct production of Cl₂

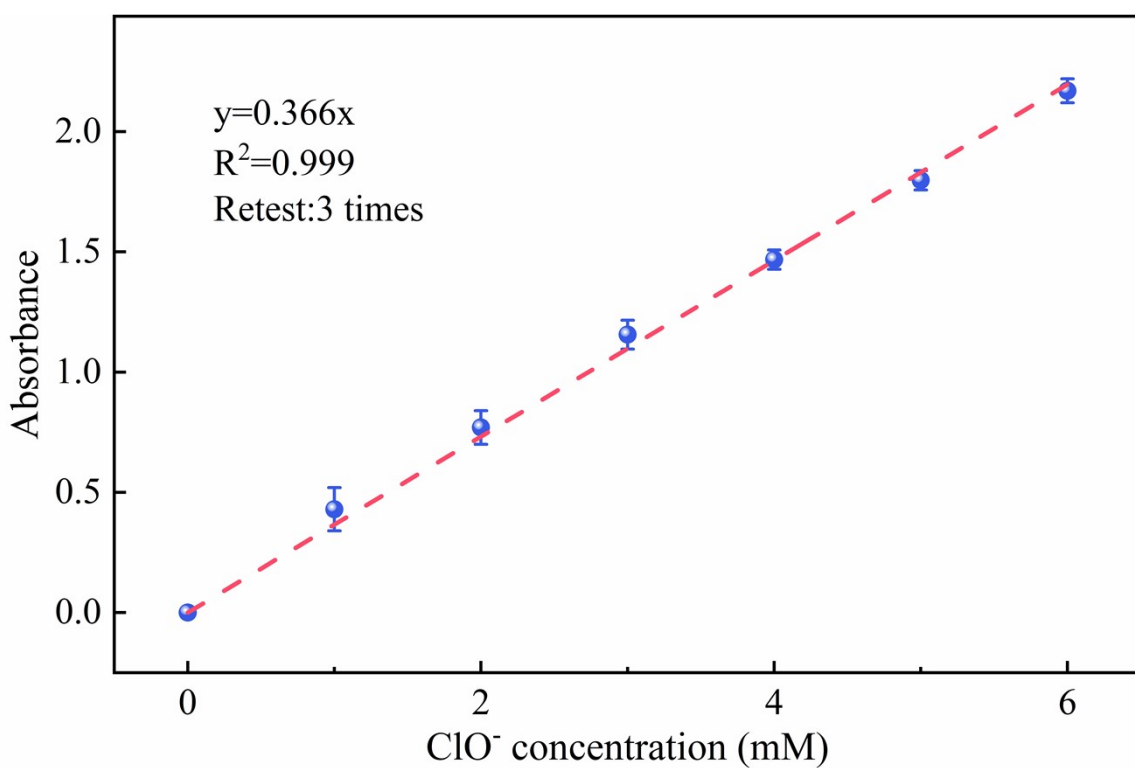
Caitao Kang, Chenglong Ding, Yao Li, Yanming Li, Changli Li*, Jingfu He*

School of Materials, Shenzhen Campus of Sun Yat-sen University, No. 66, Gongchang Road,
Guangming District, Shenzhen, Guangdong 518107, P.R. China

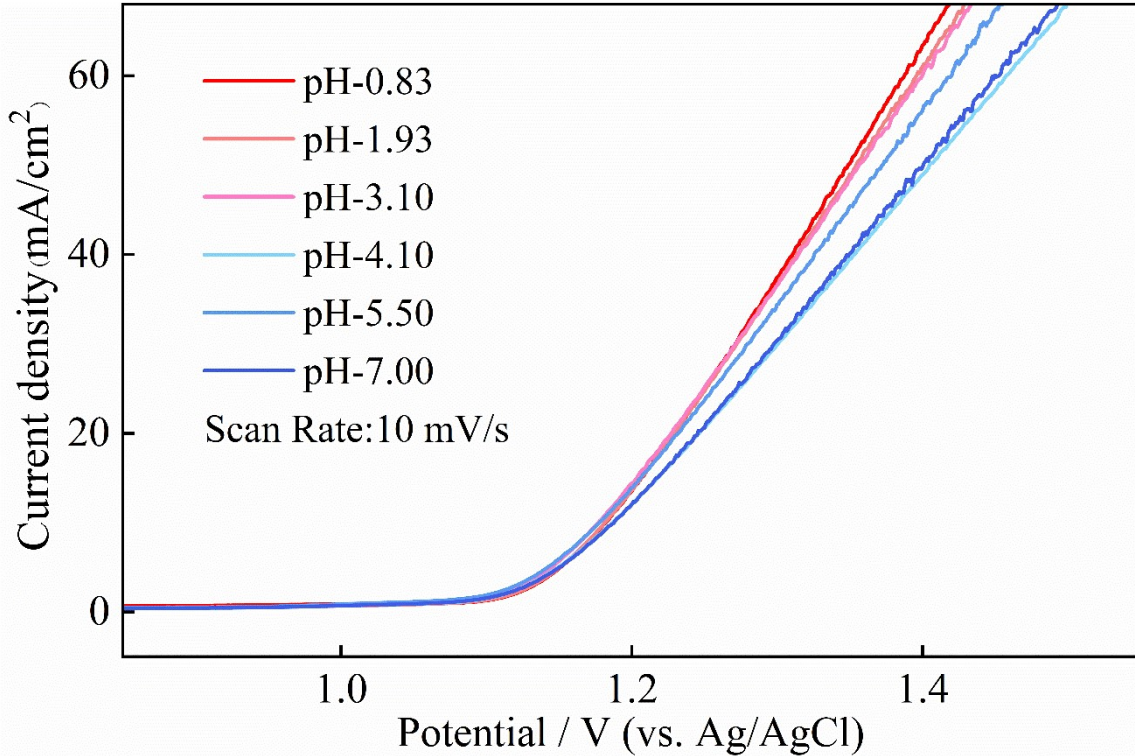
*E-mail: lichli5@mail.sysu.edu.cn; hejf27@mail.sysu.edu.cn



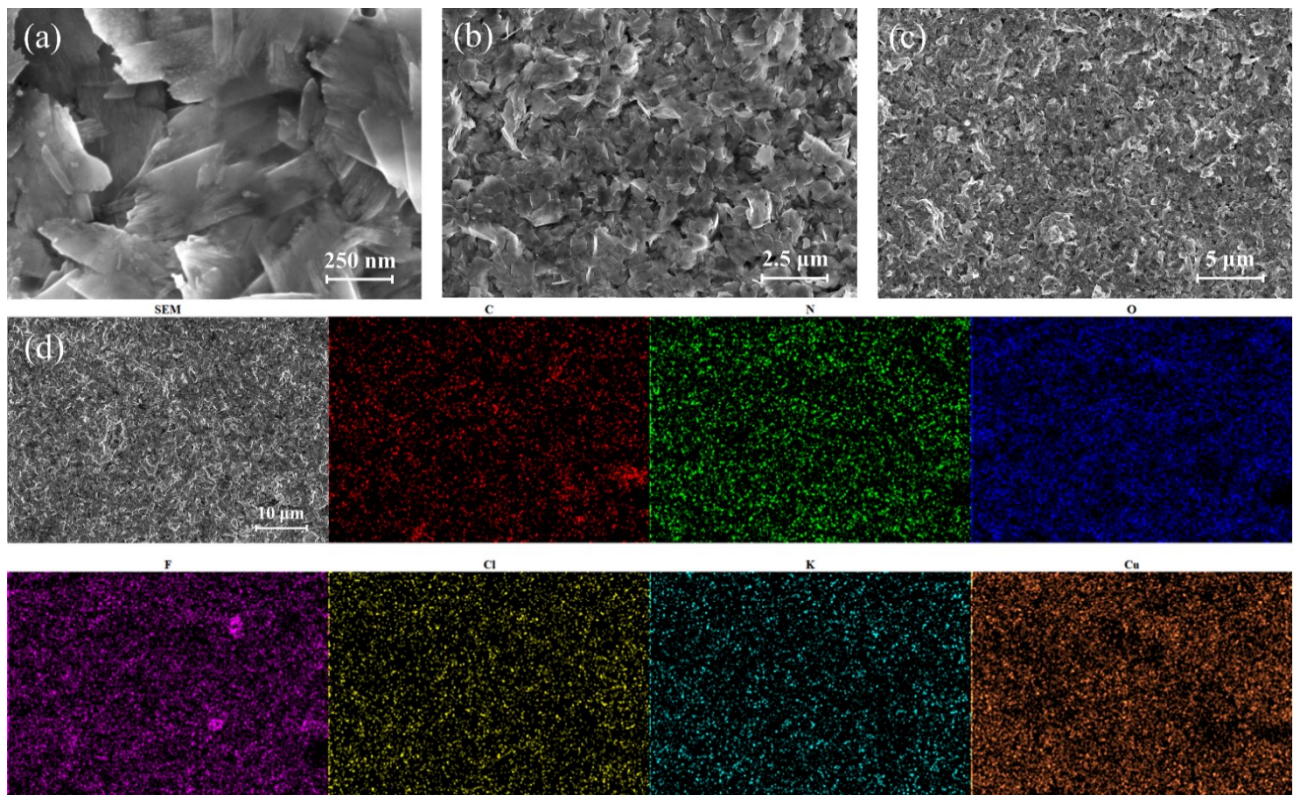
Supplementary Figure 1. The quantification of hypochlorite concentration by UV-vis.



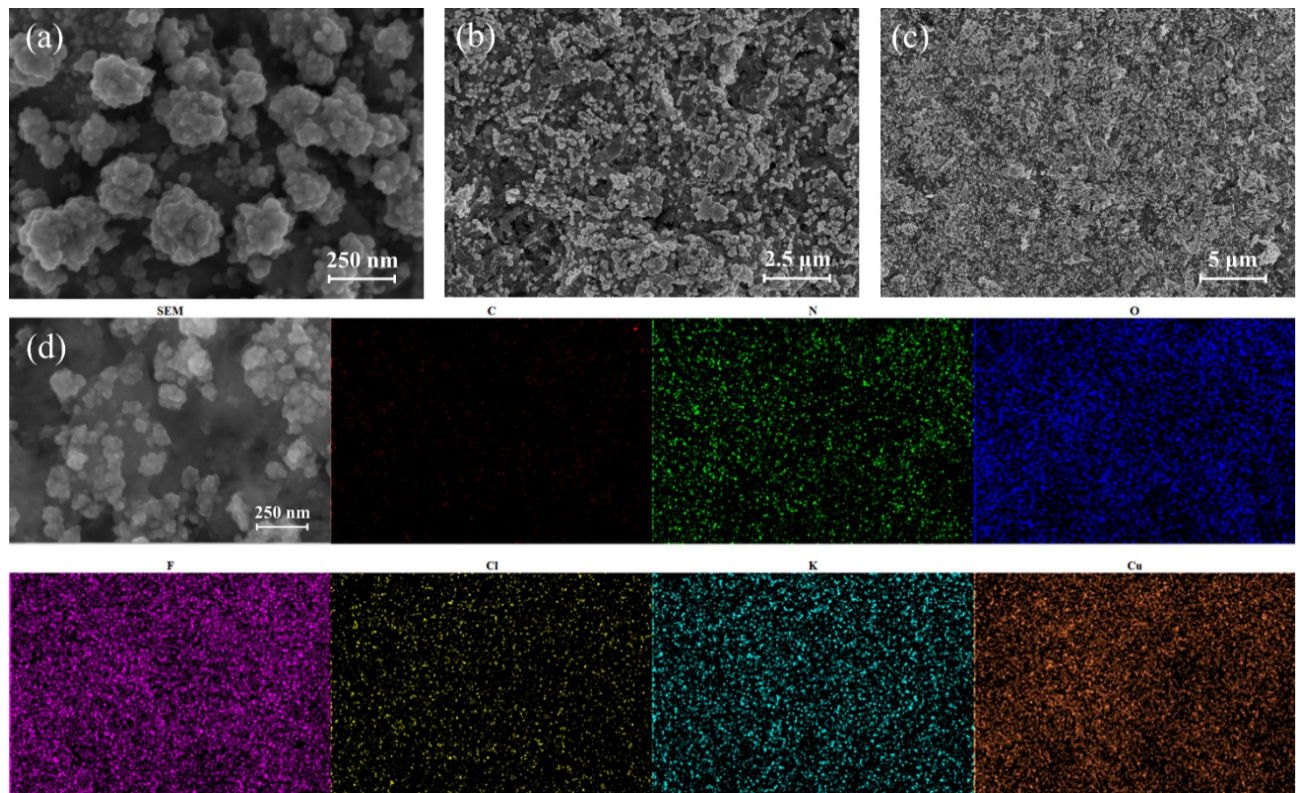
Supplementary Figure 2. ClO⁻ standard curve in 1 M KOH with 2 M KCl.



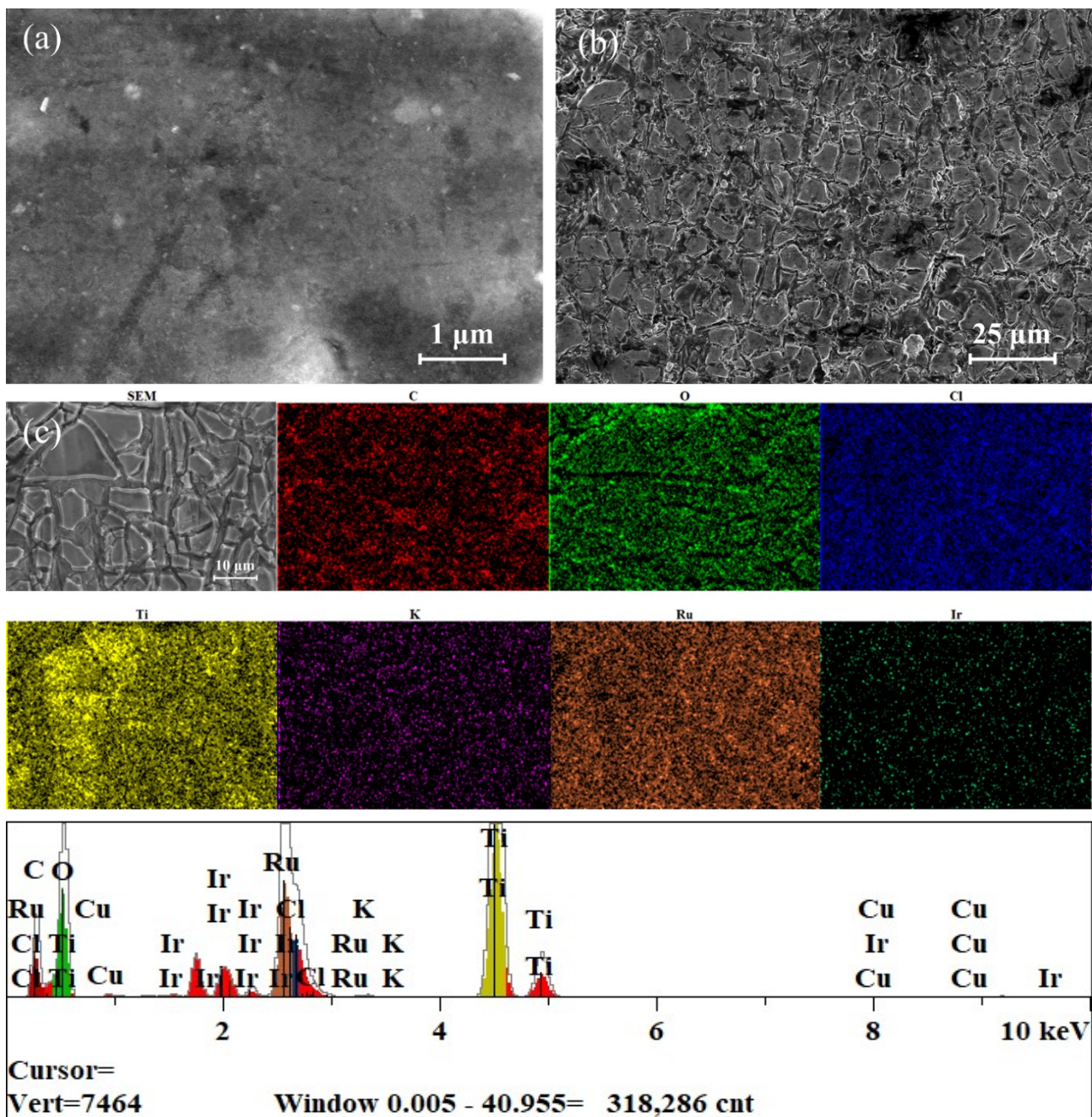
Supplementary Figure 3. Cl⁻ oxidation waves observed during linear sweep voltammetry of DSA catalyst in 2 M KCl at different pH.



Supplementary Figure 4. Surface morphology and EDS mapping images of CuO catalyst before the reaction.



Supplementary Figure 5. Surface morphology and EDS mapping images of CuO catalyst after the reaction.

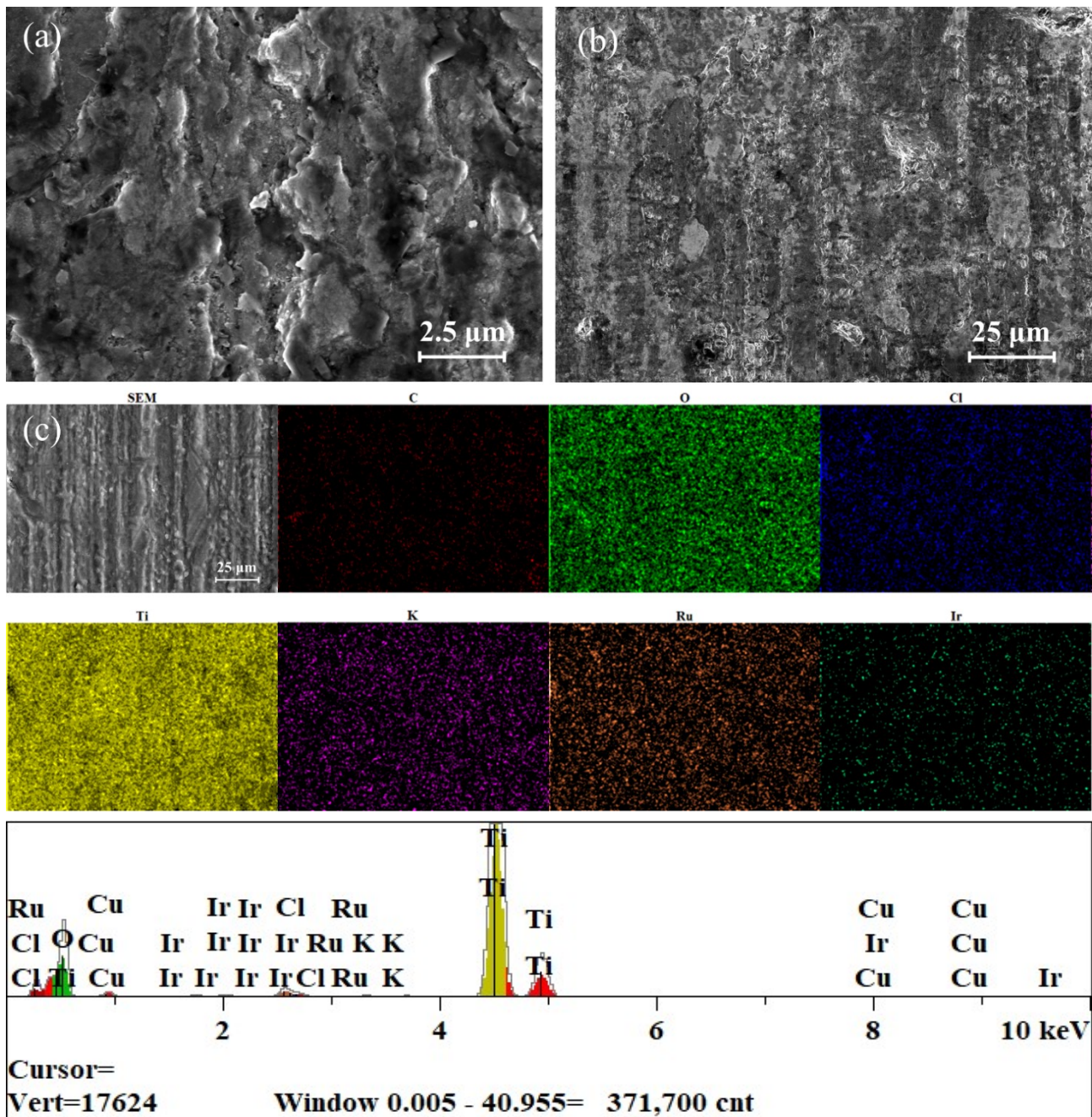


Supplementary Figure 6. Surface morphology and EDS mapping images of DSA catalyst before the reaction.

Supplementary Table 1. EDS-area mapping images of DSA catalyst before the reaction.

Elt.	Intensity (c/s)	Atomic %	Atomic Ratio	Conc.	Units	Error 2-sig	MDL 3-sig	
C	349.99	11.936	0.2181	4.454	wt.%	0.044	0.070	
O	939.47	54.729	1.0000	27.206	wt.%	0.152	0.170	
Cl	162.65	1.023	0.0187	1.127	wt.%	0.028	0.073	
K	18.77	0.142	0.0026	0.172	wt.%	0.028	0.084	
Ti	2,517.80	22.564	0.4123	33.558	wt.%	0.113	0.109	

Ru	1,237.29	8.114	0.1483	25.480	wt.%	0.136	0.221	
Ir	12.85	1.265	0.0231	7.552	wt.%	1.002	2.888	
		100.000		100.000	Wt.%			Total

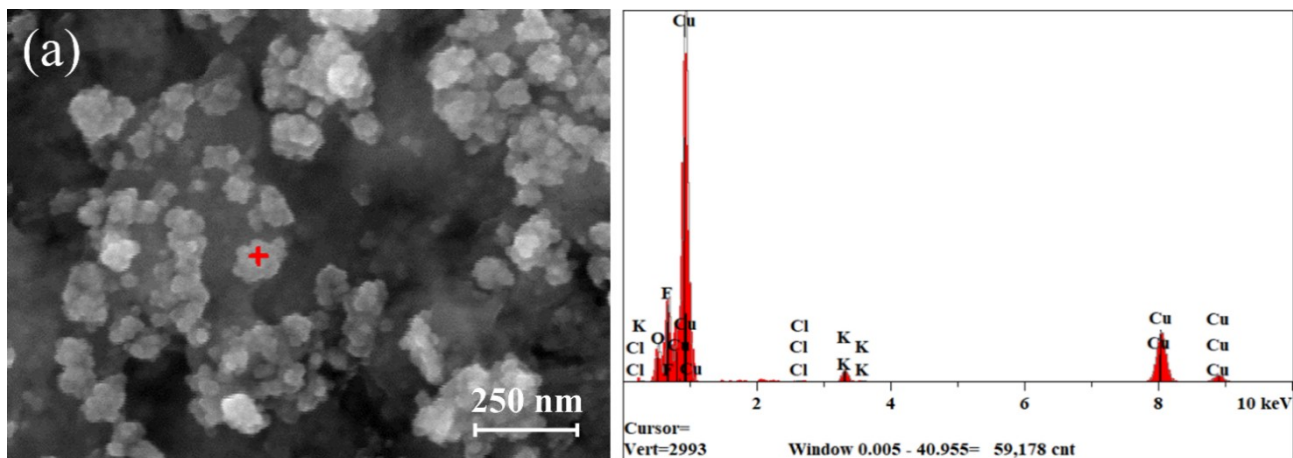


Supplementary Figure 7. Surface morphology and EDS mapping images of DSA catalyst after the reaction.

Supplementary Table 2. EDS-area mapping images of DSA catalyst after the reaction.

Elt.	Intensity (c/s)	Atomic %	Atomic Ratio	Conc.	Units	Error 2-sig	MDL 3-sig	
C	185.82	5.437	0.1008	2.199	wt.%	0.033	0.065	

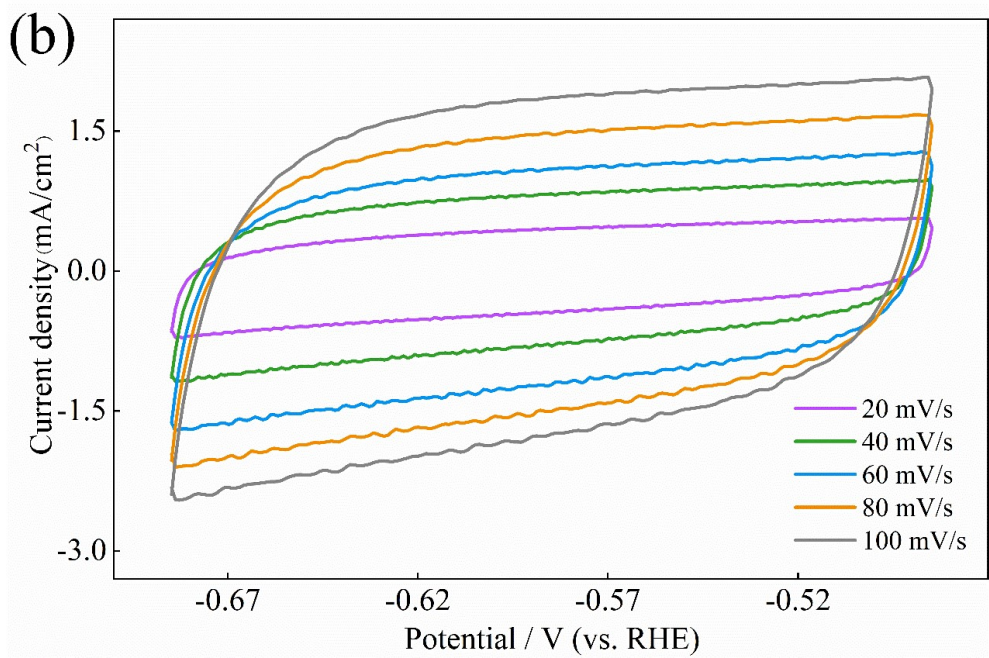
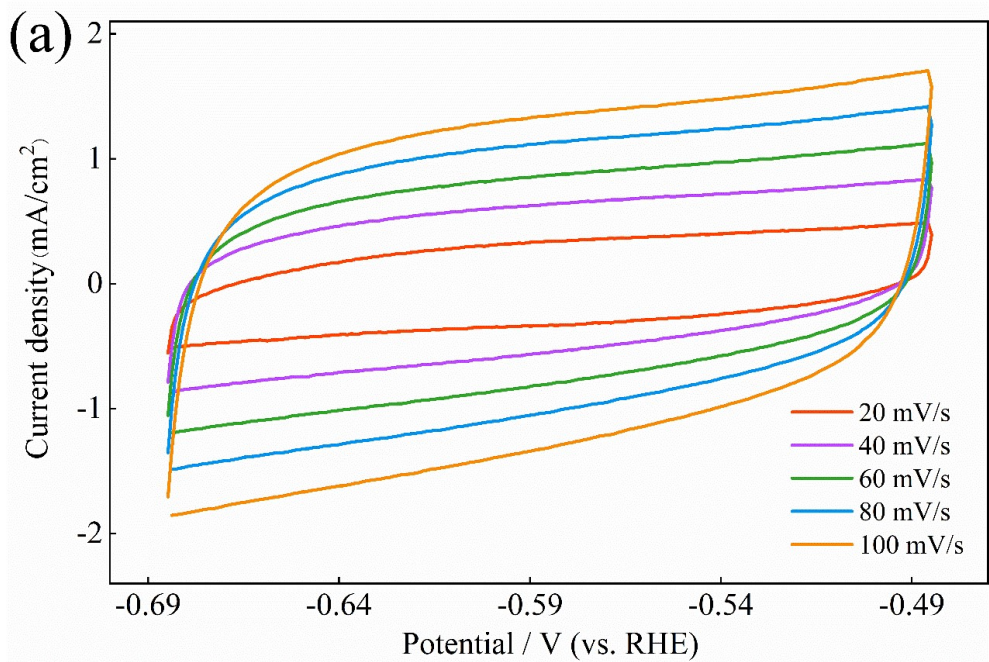
O	834.80	53.930	1.0000	29.061	wt.%	0.174	0.202	
Cl	34.91	0.161	0.0030	0.192	wt.%	0.020	0.058	
K	38.18	0.177	0.0033	0.233	wt.%	0.020	0.057	
Ti	5,918.76	38.748	0.7185	62.467	wt.%	0.133	0.088	
Ru	118.71	0.445	0.0083	1.516	wt.%	0.049	0.135	
Ir	5.84	0.455	0.0084	2.946	wt.%	0.813	2.417	
		100.000		100.000	Wt.%			Total

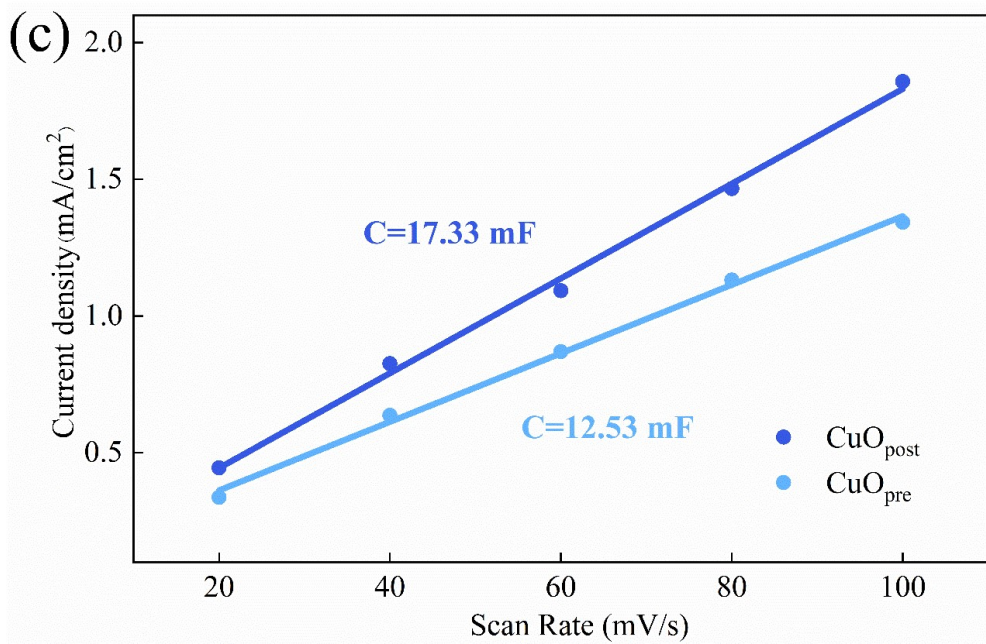


Supplementary Figure 8. Surface morphology and EDS-point mapping images of CuO catalyst after the reaction.

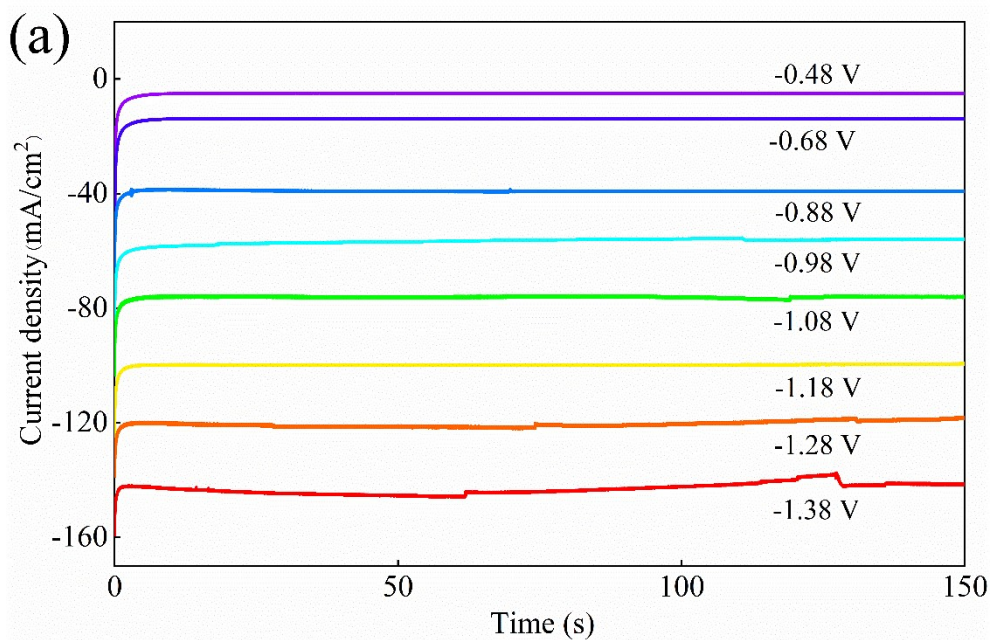
Supplementary Table 3. EDS-spot mapping images of CuO catalyst after the reaction.

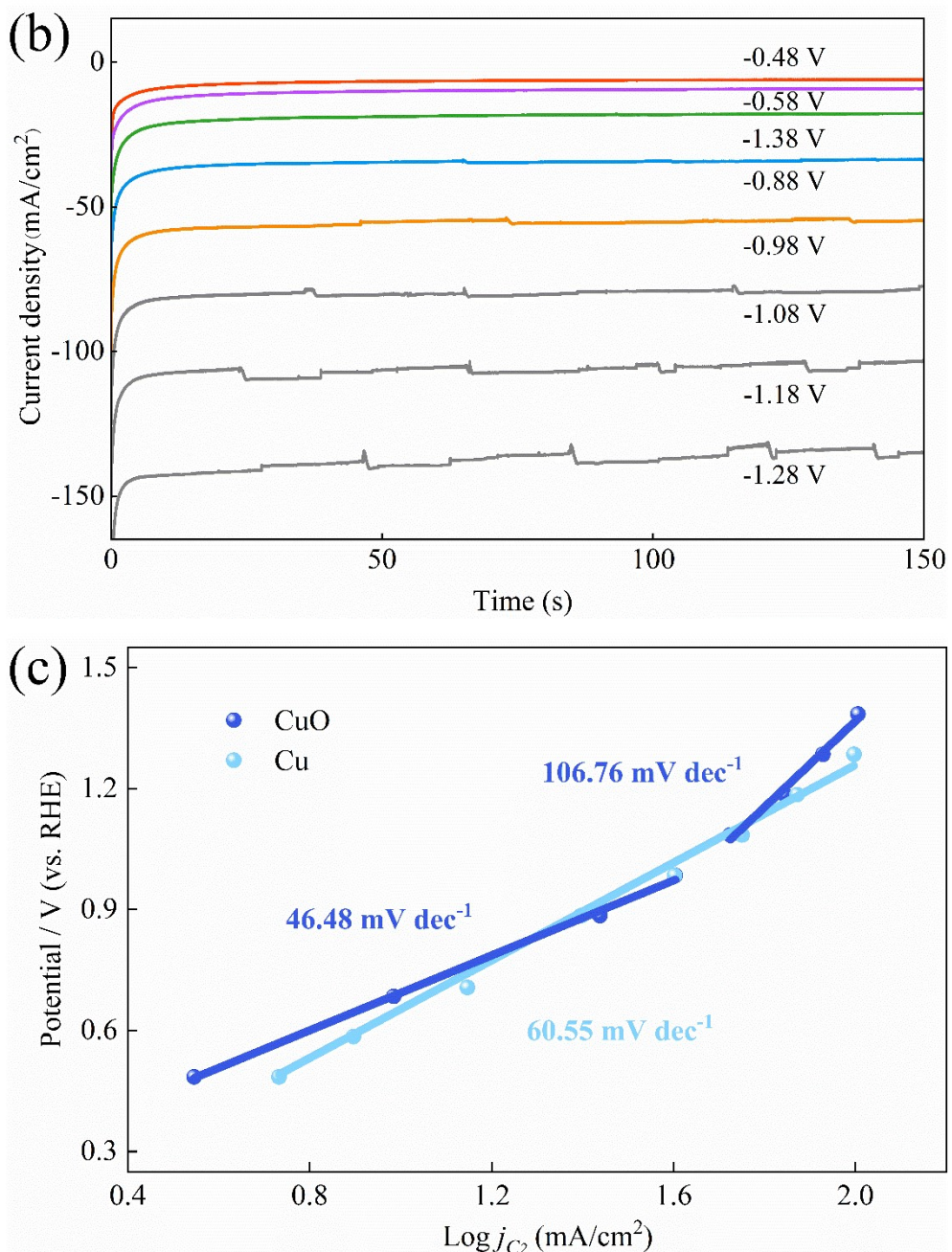
Elt.	Intensity (c/s)	Atomic %	Atomic Ratio	Conc.	Units	Error 2-sig	MDL 3-sig	
C	3.83	2.602	0.1442	0.766	wt.%	0.676	1.014	
N	1.46	0.862	0.0478	0.296	wt.%	0.507	0.766	
O	81.39	18.044	1.0000	7.074	wt.%	0.355	0.352	
F	185.17	26.517	1.4695	12.344	wt.%	0.357	0.264	
Cl	3.81	0.226	0.0125	0.197	wt.%	0.119	0.173	
K	35.43	2.094	0.1160	2.006	wt.%	0.166	0.183	
Cu	207.27	49.656	2.7519	77.318	wt.%	1.912	0.752	
		100.000		100.000	Wt.%			Total



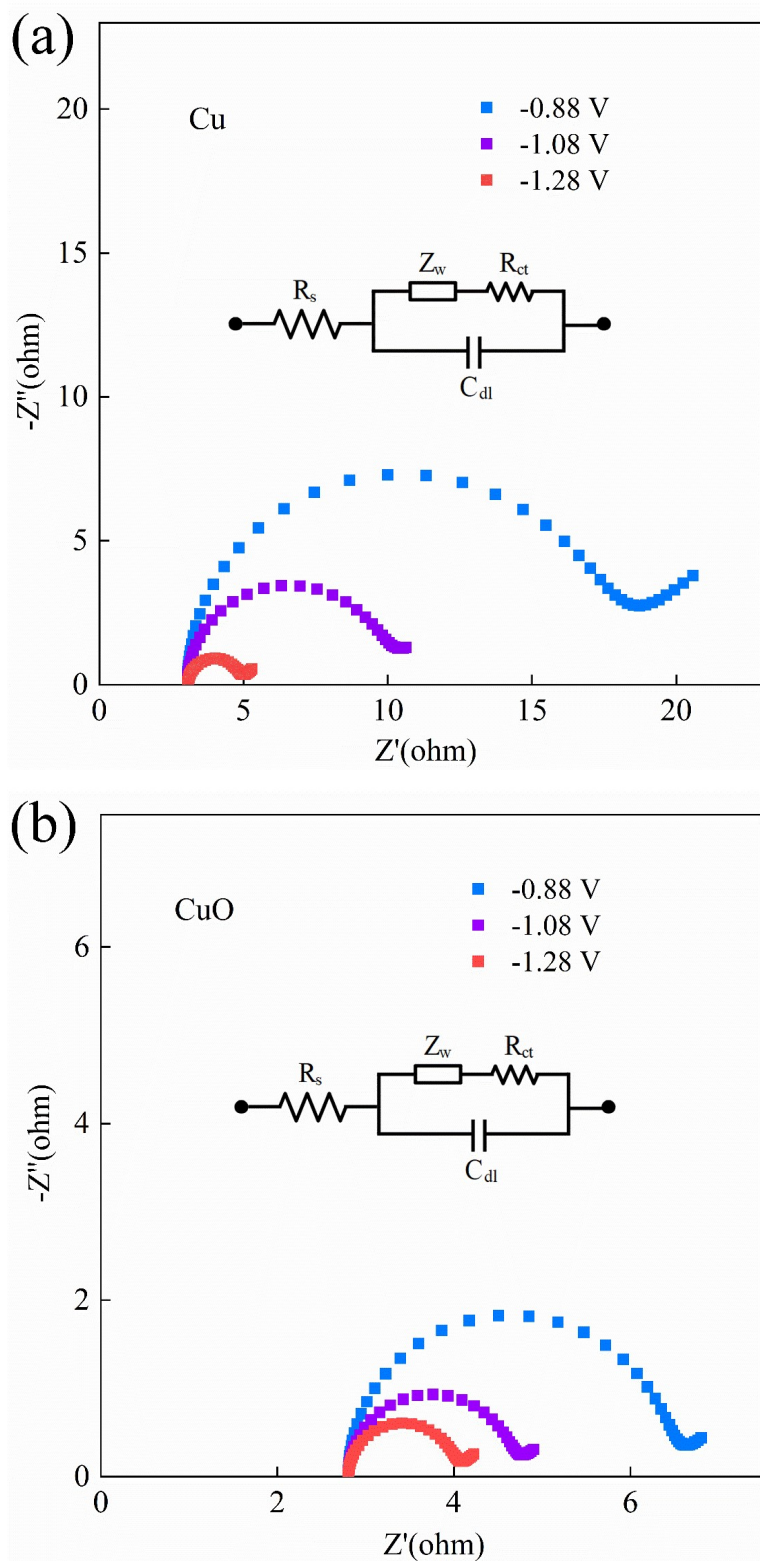


Supplementary Figure 9. Determination of double-layer capacitance for CuO catalysts before and after the reaction in 0.5 M KHCO₃. The CVs of (a) CuO before the reaction and (b) CuO after the reaction taken over a range of scan rates in a potential window where only double-layer charging and discharging is relevant. (c) Current due to double-layer charge/discharge plotted against CV scan rate.

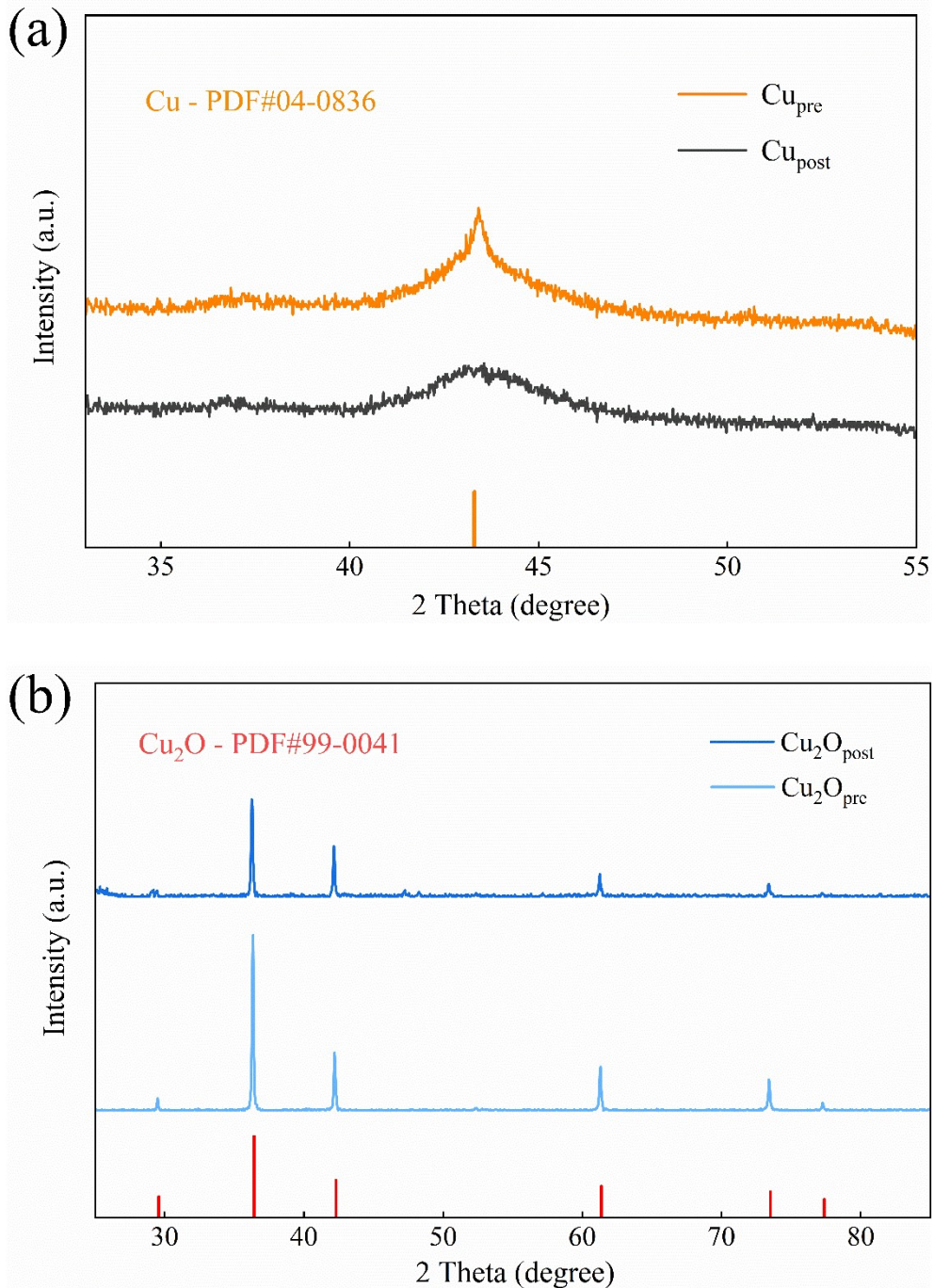




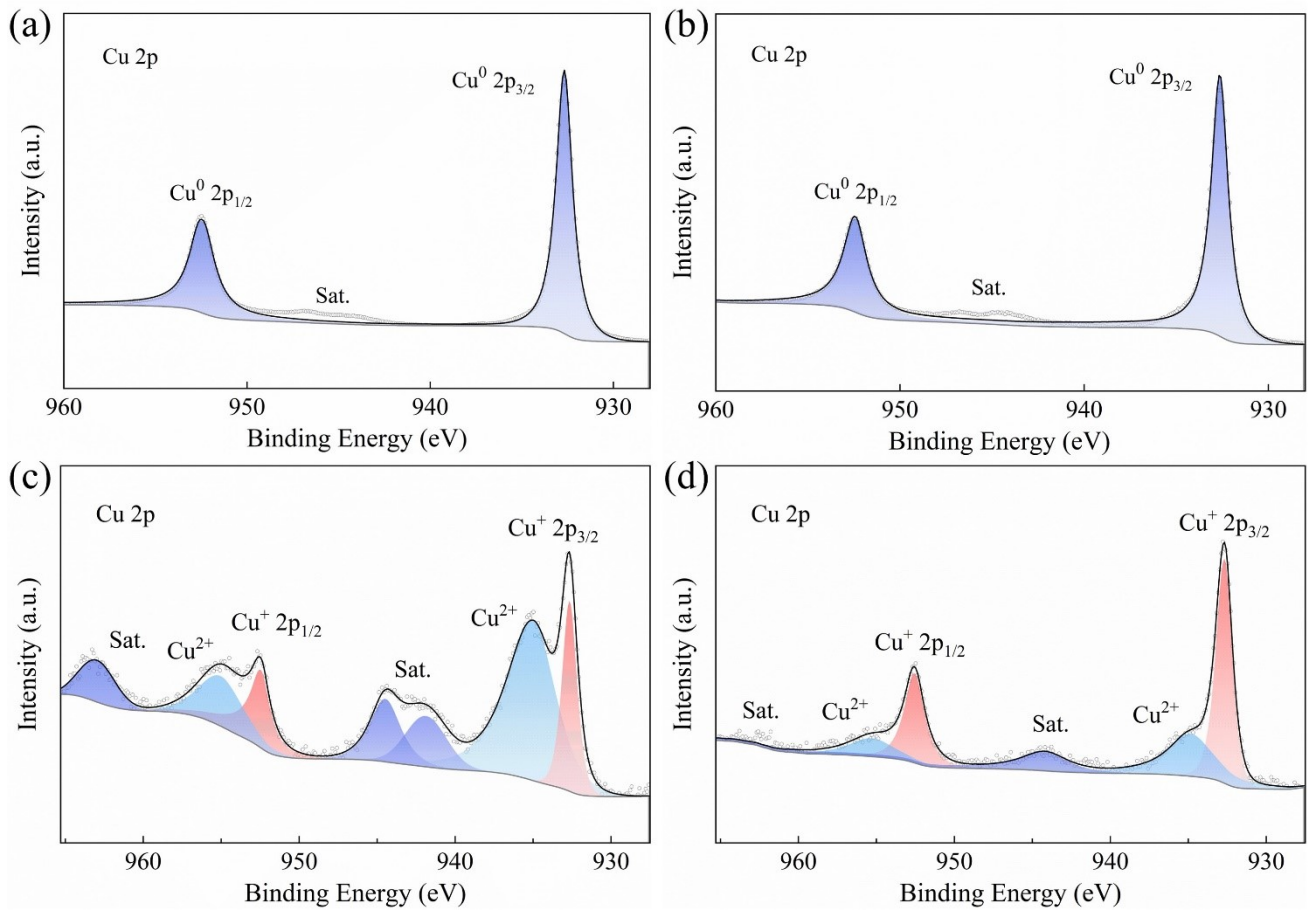
Supplementary Figure 10. CA responses of activity stabilized (a) CuO and (b) Cu catalysts in 0.01 M HCl and 2 M KCl in the catalytic turnover region. (c) True steady-state polarization curve (Tafel plot) constructed from CO₂RR current densities sampled from steady-state CA responses.



Supplementary Figure 11. Representative EIS measurements on (a) Cu and (b) CuO catalysts acquired at different potentials (reference electrode: Ag/AgCl; counter electrode: DSA; cell: floe cell; electrolyte: 0.01 M HCl and 2 M KCl).



Supplementary Figure 12. XRD patterns of (a) Cu and (b) Cu₂O catalysts over carbon cloth before and after the reaction. The standard power diffraction file (PDF) index of Cu (ICDD PDF# 04-0836) and Cu₂O (ICDD PDF# 99-0041) are plotted for comparison.



Supplementary Figure 13. XPS spectrum of the Cu catalysts (a) before and (b) after the CO₂RR. XPS spectrum of the Cu₂O catalysts (c) before and (d) after the CO₂RR.